BOLETIN DE LA SOCIEDAD ESPAÑOLA DE
Cerámica y Vidrio
A R T I C U L O

Tuned driving of piezoelectric resonators: impedance matching

J.L. PONS[1], J.F. FERNÁNDEZ[2], M.VILLEGAS[2], P. OCHOA[2], R. CERES[1], L. CALDERÓN[1], E. ROCON[1]
[1]Grupo de Bioingeniería, Instituto de Automática Industrial, CSIC, Ctra. Campo Real, km. 0,200,28500 Arganda del Rey, Madrid
[2]Instituto de Cerámica y Vidrio, CSIC, Camino de Valdelatas s/n, 28049 Madrid

For optimal operation of piezoelectric resonators, the electrical impedance of electronic drivers and the resonator itself must be matched. Lack of matching results in a non smooth transmission of electrical power between the drive and the load which, in turn, leads to heating and poor efficiency. The rest of properties of the driving voltage (frequency, amplitude and phase) are also affected by this mismatch. This paper presents the optimal design of power drivers for piezoelectric resonators. This approach is based on a first stage of electro-mechanical experimental characterization. This first step sets the basis for an impedance matching process. The approach has been experimentally validated on a well known piezoelectric resonator: the ultrasonic motor.

Keywords: Piezoelectric resonators, mechatronic design, ultrasonic motors, impedance matching.

Sintonización de resonadores piezoeléctricos: Ajuste de impedancia.

La operación óptima de un resonador piezoeléctrico requiere de la adaptación de impedancia eléctrica entre el circuito de excitación y el propio resonador. La falta de adaptación se traduce en una pobre transmisión de potencia desde el excitador hasta el resonador, lo que a su vez se traduce en calentamiento y pérdida de eficienca en la operación. Las características morfológicas de la tensión de excitación (amplitud, frecuencia y fase) también quedan afectadas por esta falta de adaptación. Este artículo analiza el diseño óptimo de la etapa de potencia de un circuito eléctrico de excitación para resonadores piezoeléctricos. Se trata la caracterización electromecánica del resonador y, en base a ésta, la adaptación de impedancias entre circuito y resonador. La contrastación experimental se ha llevado a cabo con un resonador bien estudiado en la literatura: un motor ultrasónico.

Palabras clave: Piezoeléctricos, diseño mecatrónico, motores ultrasónicos, adaptación de impedancia.

1. INTRODUCTION

Ultrasonic motors are specific instances of resonant electromechanical structures. A piezoelectric disc (alternatively poled) is responsible for exciting an electromechanical vibration in the vicinity of resonance or antiresonance. As a consequence, the ultrasonic motor as a whole can be considered a piezoelectric resonator.

The intrinsic electromechanical nature of these drives calls for a concurrent engineering approach in which various disciplines are required to ensure an optimal design and implementation. This is the so-called mechatronic approach to system development, (1).

The design of feedback control loops in the control electronic circuit for these drives has been analyzed in detail by the authors, (2). However, additional aspects must be taken into consideration when attempting a comprehensive mechatronic approach to the design of efficient and robust electronic power drivers for these motors. A very important and interesting issue of this mechatronic approach is that of optimizing the power stage of driving electronic circuits, (3), (4).

Whenever the electrical impedance of an electronic driver and the one of the load (the ultrasonic motor in this paper) are not conveniently matched, the flow of energy from the drive to the load is not smooth. Part of the driving power from the power electronic driver is lost in the process of heating and this inevitably results in reduced efficiency. In most cases, this process is accompanied by a low quality in the power signal which can be seen in the undesired presence of harmonics, reduced voltage amplitude and phase lags.

This paper can be seen as a complementary work of (2). In (2), the main topic is the tracking of resonance frequency. This paper will specifically address the power transmission between the power electronic driver and the piezoelectric resonator through a process of impedance matching. In a first section, we will concentrate on the electromechanical characterization of the piezoelectric resonator as a preliminary step in the process of impedance matching. The next section will then focus on designing power electronics according to the load. The experimental validation of the proposed method has been implemented on a comercial ultrasonic motor for which the results are given and discussed.

2. ELECTROMECHANICAL ANALYSIS

The electromechanical analysis of a load can be seen as a necessary preliminary step when electrical impedance matching between the power driver and the load is required. The electrical impedance matching between both components has a direct effect on the quality of the electrical power signal

used to drive the piezoelectric resonator. The reduced quality refers here to the inclusion of undesired frequency harmonics, the morphology of the signal, its amplitude and phase lag in the case of multiple phase loads (as in the case of ultrasonic motors). The immediate consequence of this mismatch is an increase in the electrical power and a non-smooth operation.

As a result of this, the electromechanical analysis and characterization of the piezoelectric resonator will be instrumental to obtain the electrical parameters of the load which will lead the process of optimizing the design of power electronic circuits to drive the resonator.

In the following sections, we will assume that the piezoelectric resonator can be modelled in the vicinity of resonance (and antiresonance) according to the equivalent electrical circuit approach. In this equivalent electrical circuit approach, C_0 is the clamped capacitance, while ,R_m L_m and $C_m$represent the motional electrical resistance, inductance and capacitance respectively.

The electrical characterization of the piezoelectric resonator will start from the analysis of the Nyquist diagram in the vicinity of resonance. In order to do so, a precision impedance meter is used to properly determine the resonator's conductance and susceptance. This data can be used to determine the Nyquist diagram for the resonator according to figure 1.

$$Y = G + jB \quad [1]$$

From the Nyquist diagram it is possible to determine a series of relevant points which are in close relation with the equivalent electrical circuit parameters, (5):

1. Determination of the clamped capacitance, C_0. In the Nyquist diagram, the maximum value of the conductance takes place at the series resonance frequency, ω_s. The susceptance at this point, $|Y_{d0}|$, is related to the clamped capacitance through the following equation:

$$C_0 = \frac{|Y_{d0}|}{\omega_s} \quad [2]$$

2. Determination of the quality factor, Q. In this case we start from the frequencies that maximize and minimize the susceptance, ω_1 and ω_2 respectively. From these two frequencies, the quality factor, Q, can be worked out according to the following equation:

$$\Delta\omega = \omega_2 - \omega_1 \quad [3]$$

$$Q = \frac{\omega_s}{\Delta\omega} \quad [4]$$

3. Determination of the motional impedance. As it was introduced above, the motional impedance consist in resistive, capacitive and inductive terms. The motional resistance, R_m, can be obtained from the maximum conductance according to the following relation:

$$R_m = \frac{1}{G_{\max}} \quad [5]$$

The motional inductance is determined from the resonance frequency, ω_s, and the modulus of the admitance, Y_{m0} , at this point:

$$L_m = \frac{1}{\omega_s \cdot Y_{m0}} \quad [6]$$

Eventually, the motional capacitance can be easily found from the resonance frequency and the corresponding inductance:

$$C_m = \frac{1}{\omega_s^2 \cdot L_m} \quad [7]$$

The various different key point in the Nyquist diagram are clearly indicated in figure 1. The previous analysis is general and can be applied to any piezoelectric resonator, be this a piezoelectric transformer, a sensor or an actuator. In this paper we used, without loss of compliteness, commercial ultrasonic motors as a particular instance of piezoelectric resonator. Shinsei USRM60 ultrasonic motors have been widely analyzed in the literature, therefore they are particularly valid to test and validate the design and optimization procedure hereby introduced. According to the manufacturer's datasheet, the main features are summarized in table I.

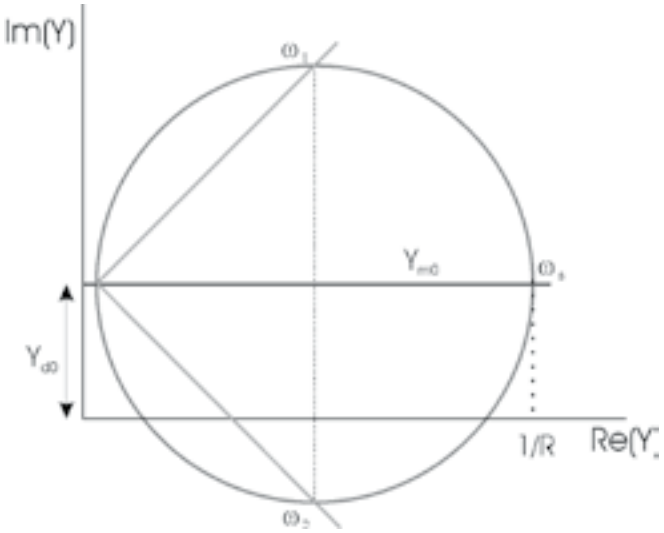

Fig. 1- Nyquist diagram used to obtain the ultrasonic motor's electrical parameters.

TABLE I. SHINSEI USRM30 AND USRM60 TECHNICAL DATA

	USRM60
Frequency	40 kHz
Driving voltage	120 V_{rms}
Torque	0.5 Nm
Power	5 W
Rotational speed	100 rpm
Stall torque	1 Nm
Vibration mode	9

The particular case of the URSM60 is well know in the scientific literature, its vibration modes are clearly identified and the driving frequency is well established. In a general case of a piezoelectric resonator where there is no previous information on vibration modes, the study would start from an electrical analysis to determine the resonance frequency of interest. Once this parameter has been determined, a mechanical modal analysis would provide additional

information on the particular vibration mode corresponding to the resonance frequency. Even though for the case of an USRM60 ultrasonic motor this preliminary electromechanical study would not be necessary, for the sake of completeness, an electromechanical analysis has been performed on this motor. With the help of a modal analysis platform, the various different vibration modes and the corresponding resonance frequencies have been computed for the USRM60 ultrasonic motor, see figure 2.

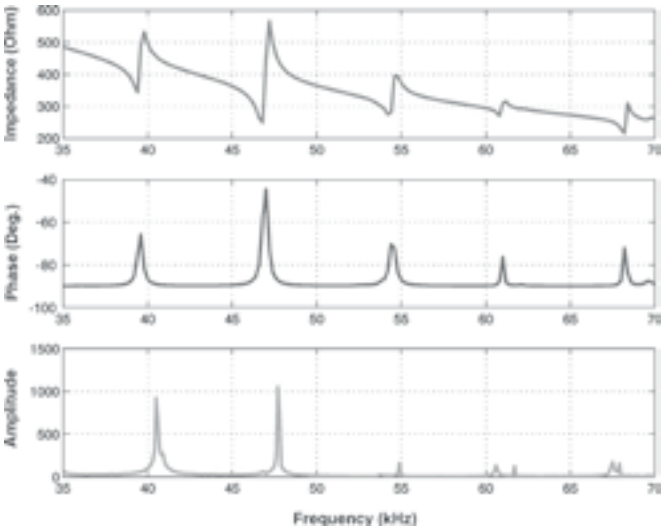

Fig. 2- Experimental electrical analysis of a commercial USRM60 ultrasonic motor.

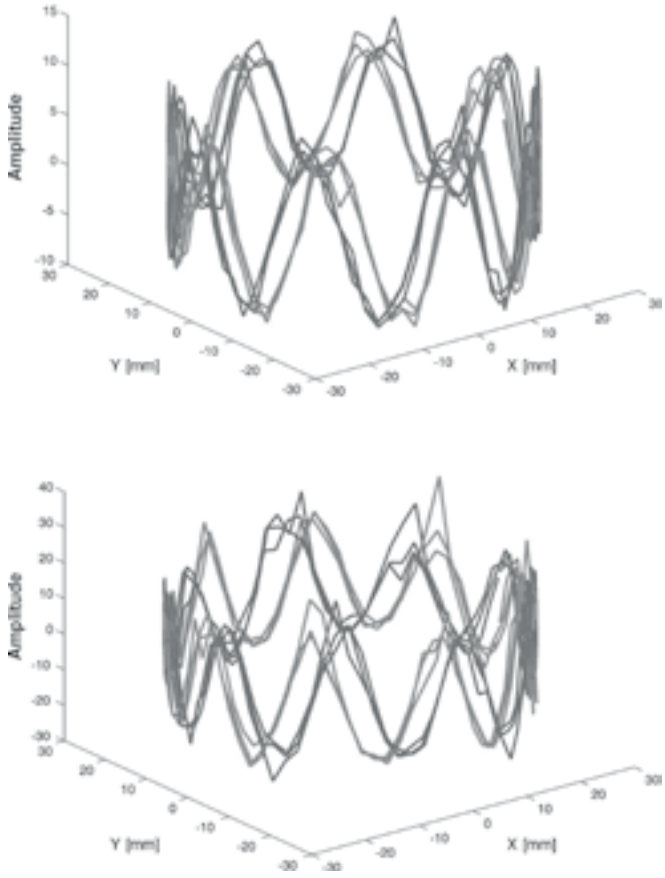

Fig. 3- Experimentally determined vibration modes (9th and 8th) of USRM60 ultrasonic motor.

After this electromechanical analysis it can easily be found that the operation mode for the USRM60 ultrasonic motor is the 9th circumferencial mode which approximately corresponds to a modal frequency of 40 kHz. These results are in full agreement with the manufacturer's data. Figure 3 shows the results of the modal analysis for two of the modal shapes. It can be easily seen that the modal shapes corresponding to the two phases (blue and red lines) are in quadrature, therefore their combination results in a travelling wave being established in the motor stator.

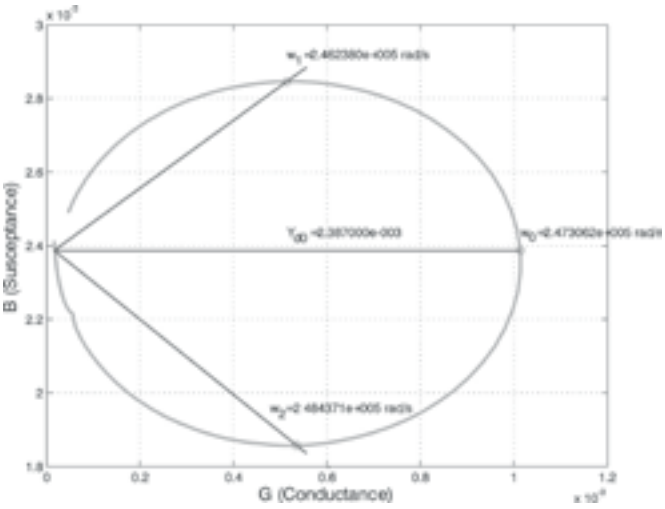

Fig. 4- Nyquist diagram of USRM60 ultrasonic motor in the vivinity of the 9th vibration mode.

Once the modal parameters are identified, it is possible to obtain the electrical paremeters as above described. Figure 4 shows the USRM60 susceptance versus conductance graph of the 9th vibration mode. By direct application of equations (1) to (7) to this experimental data, the different electrical parameters for the motor are determined. Table II shows the electrical parameters of the equivalent electrical model for the USRM60 ultrasonic motor.

TABLE II. ELECTRCAL PARAMETERS FOR THE EQUIVALENT ELECTRICAL CIRCUIT MODEL OF A SHINSEI USRM60 ULTRASONIC MOTOR.

	C_0	f_s	Q	R_m	L_m	C_m
Phase 1	9.2 nF	39519 Hz	95	1136 Ω	435 mH	37.3 pF
Phase 2	9.6 nF	39485 Hz	73.3	1083 Ω	320 mH	50.8 pF

In order to verify the validity of the equivalent electrical model for the USRM60 ultrasonic motor, figure 5 represent the experimental values for the electrical impedance and the phase lag in the vivinity of the 9th modal frequency and the simulation of this values based on the proposed equivalent electrical circuit and the experimentally determined electrical parameters..

3. DESIGN AND IMPLEMENTATION OF THE POWER STAGE

In this section we will address the optimal design of a

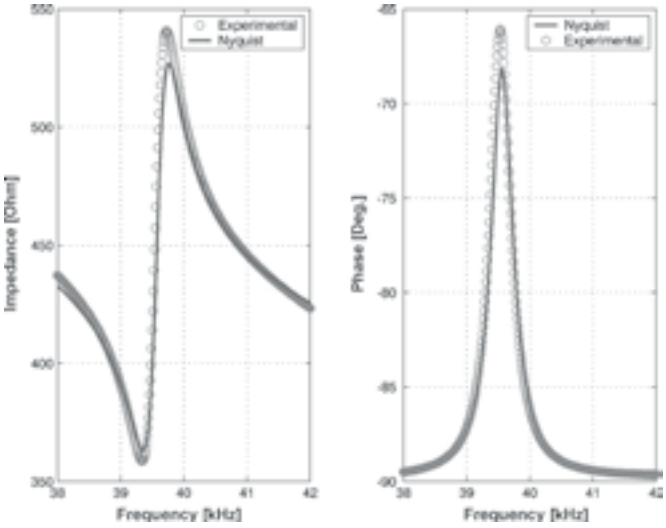

Fig. 5- Comparision between experimental and simulated frequency behaviour of the USRM60 ultrasonic motor for the 9th vibration mode.

power stage for a piezoelectric resonator. This electrical stage is in charge of rising the power and voltage level from the control signals. In this stage we assume that proper and tuned control signals have been provided by a previous electronic stage. These control signals meet the following criteria, (2):

1. They are tuned to the resonance frequency of the ultrasonic motor and a perturbation rejection control loop has been implemented to ensure optimal driving conditions.

2. They are switched signals with a proper selection of duty cycle to allow low content of harmonics.

The power stage comprises a "push – pull" transformer and two resonant LC circuits that help rise both the power and voltage level of the control signals. By using the "push – pull" configuration for the power transformers, the transormer ratio is minimized and only a low voltage at the primary windings is required. The design primary voltage for this configuration is 36 V and should be adjustable for an easy control of the amplified voltage level.

The resonant converters are analogue electrical circuits usually applicable in the power stages of control circuits for travelling wave ultrasonic motors, see figure 6. If the output voltage of the switched control signal would be directly applied to the load (the motor phases), high current spikes would be produced due to the motor's clamped

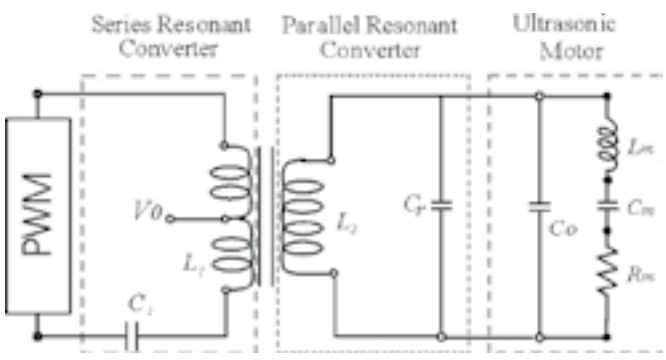

Fig. 6- Schematic representation of the power stage and series and parallel resonant converters.

capacitance, C_0. This problem can be avoided by properly using an inductance (L_1) in series with the load. However, this inductance, in addition of lowering the harmonic content in the power signal, would also limit and reduce the voltage level at the fundamental driving frequency. This undesired voltage drop at the fundamental frequency can be compensated for by using a second capacitance (C_1) in series with L_1. Both L_1 and C_1 implement a resonant series filter as depicted in figure 6. The series capacitance (C_1) plays a secondary role in this power stage, in addition of setting up a series resonant filter, it contributes to filter out any low frequency component at the input of the power stage.

The condition of impedance matching between the power stage and the load requires that the resonant frequency of the series resonant filter and that of the load be the same. This condition is mathematically expressed according to the following equation:

$$L_m C_m = L_1 C_1 \qquad [8]$$

When this condition is met, the power transmission between the power stage and the load is maximized. In addition to this resonant series filter, it is commonly included in the design of the power stage a seccondary parallel resonant circuit. This resonant circuit comprise an inductance in parallel with the load (L_2) and a capacitance (C_r), see figure 6. This seccondary inductance serves to compensate the reactive electrical current due to the motor's clamped capacitance, C_0. Again, it is convenient to fix the resonance frequency of this seccondary resonant circuit at the same frequency that the motional resonance frequency of the load. This condition reads:

$$L_m C_m = L_2 \left(C_0 + C_r \right) \qquad [9]$$

Since we use a transformer in our power stage for voltage amplification, the primary and seccondary windings of this transformer could be used as the inductance for the series and parallel resonant converters. In the case of the seccondary parallel converter this implies matching the seccondary winding inductance to L_2. However this is a complex task that, in general, needs the following two steps:

1. In case the resonance frequency of the resonant parallel converter is lower than desired (or what is the same, the seccondary winding inductance, L_2, is too high), a shunt inductance (L_p) can be used:

$$L_p \| L_2 = \frac{L_2 \cdot L_p}{L_p + L_2} \qquad [10]$$

2. In the case the resonance frequency of the resonant parallel converter is higher than desired (or what is the same, the seccondary winding inductance, L_2, is too low), a shunt capacitance (C_1) can be used:

$$C_1 \| C_r = C_1 + C_r \qquad [11]$$

If we follow the approach of using the primary and seccondary windings of the transformer as the series and parallel inductances respectively, L_1 and L_2 represent the inductance of these windings. Under this approach, the condition for optimized power transmission between the power stage and the piezoelectric resonator can be given by:

$$L_m C_m = L_2 (C_0 + C_r) = L_s C_1 \quad [12]$$

In equation [12] the inductance of the series resonant filter is the leakage inductante of the transformer, that for the primary winding is:

$$L_s = L_1 - \frac{M^2}{L_2} \quad [13]$$

where M is the transformer's mutual inductance.

When working out the values of the power electronics series and parallel resonant converters (L_s, L_2, C_1 and C_r) additional retrictions apply. In particular, in addition to the fundamental resonance frequency, f_r, two parasitic resonant circuits can be found. These are mainly due to the high flux of recative current in the power stage. The first parasitic resonant electrical circuit comprise the series conductance, C_1, and the transformer's primary winding inductance, L_1. Since L_1 will always be higher than the leakage inductance, L_s, (see equation [13]), the resonance frequency of this parasitic circuit will always be lower than the fundamental resonance frequency of the piezoelectric resonator. Under these conditions, the parasitic resonance will only be excited in transient operation, for instance when switching the power stage on.

The second parasitic electrical circuit comprises the leakage inductance, L_s, and the series connexion of C_1 and C_0+C_2. The resonance frequency of this second parasitic circuit is higher than the piezoelectric resonator's resonance frequency. The only feasible way of limiting the effectt os this second parasitic resonance is by limiting the harmonic content of the control signal. The approach to limit harmonics in switched signals has been analyzed in detail somewhere else, (2, 6). Basically consist in selecting symmetrical bipolar switched control signals for which even harmonics vanish. In such a case, an additional condition must be imposed on the power stage. This condition sets the minimum value of the second parasitic resonance frequency to $2f_r$. Mathematically this can be formulated according to the following equation:

$$C_0 + C_r > \frac{C_1 L_1}{\sqrt{3} L_2} \quad [14]$$

Ir is convenient to note that when designing power transformers, all three relevant inductances, i.e. L_1, L_2 and L_s, can be individualy adjusted. The reason for this is in the fact that for a given transformer all the involved inductances depend directly on the squared winding turns. In addition, for a transformer, both L_1 and L_2 depend on the transformer's core air gap, however this is not the case for the leakage inductance, L_s. Therefore, when designing a power transformer, there are three degrees of freedom, the primary winding turns, the seccondary winding turns and the core's air gap. These three parameters can be used to independently adjust the three inductances. In so doing, it has to be taken into account that two of the inductance parameters, L_1 and L_2, are related through the transformer's gain.

The various different design parameters as worked out for the transformers in the power electronic stage for the USRM60 ultrasonic motor are summaruzed in Table III.

The design data of Table III, the electrical characterization of the resonant converters (L_1 and L_2), see Table IV, and equations [12] through [14] it is possible to work out all the different design parameters for the power stage. In particular, all the electrical parameters required to establish the parallel resonant converted can be found in Table V.

TABLE III. TRANSFORMER PARAMETERS AFTER IMPEDANCE MATCHING

Specifications	Data	Specifications	Data
Trafo Core	RM-10	Primary turns	20
Frequency	40 kHz	Seccondary turns	130
Primary Voltage	11.62 V_{rms}	Joule losses	0.28 W
Primary current	2 A	Core losses	0.34 W
Seccondary Voltage	75 V_{rms}	Efficiency	97.22
Seccondary current	0.31 A	Primary wire	HF-25
Power	23.41 W	Seccondary wire	HF-34

As it can be seen in Table IV, an inductance (L_p) is used in parallel to the seccondary winding of the transformer. This is due to the fact that the theoretical inductance (L_2 Theoretical) required is lower than the seccondary winding inductance (L_2 Experimental). By using this inductance, the overall parallel inductance is reduced until it is tuned to the piezoelectric resonator. The process to design the series resonant converter is simmilar and the corresponding electrical parameters are indicated in Table V.

TABLE IV. ELECTRICAL DATA FOR THE TRANSFORMER'S PRIMARY AND SECCONDARY WINDINGS

Transformer	L_1	L_2
RM3-B	0.26 mH	10.10 mH
RM3-C	0.27 mH	10.18 mH

TABLE V. ELECTRICAL PARAMETERA OF THE PARALLEL RESONANT CIRCUIT

	$L_m C_m$	C_0	L_2 (Theoretical)	L_2 (Experimental)	L_p
Phase 1	16.22 10^{-12}	9.2 nF	1.76 mH	10.10 mH	2.13 mH
Phase 2	16.25 10^{-12}	9.6 nF	1.69 mH	10.18 mH	2.02 mH

TABLE VI. ELECTRICAL PARAMETERA OF THE PARALLEL RESONANT CIRCUIT

	$L_m C_m$	L_1	C_1
Phase 1	16.22 10^{-12}	0.26 mH	62.38 nF
Phase 2	16.25 10^{-12}	0.27 mH	60.18 nF

In addition to determining the capacitance in the series resonant converter (C_1), care must be taken to ensure that equation [14] is met for this design.

$$C_1 < \sqrt{3}\frac{L_2}{L_1} C_0 \qquad \begin{cases} \text{Phase 1} \rightarrow 0.62\ \mu\text{F} \\ \text{Phase 2} \rightarrow 0.62\ \mu\text{F} \end{cases} \quad [15]$$

4. EXPERIMENTAL RESULTS

The validation procedure for the proposed design methodology will be based on the analysis of how the matched power stage affects the quality of the power signals to drive the piezoelectric resonator as compared to unmatched power drives.

For the particular case of an USRM60 ultrasonic motor, the design procedure for the power stage of the electronic driver has been applied to both motor phases. As we indicated in

a previous section, we focus here on the power stage and assume that the control signals have been properly provided, in particular we assume that the fundamental frequency of the control signal matches the resonance frequency of the piezoelectric resonator (each motor phase). Therefore, we will only focus here on studying the power signals in terms of phase lag (between phases) and amplitude.

Figure 7 shows a comparison between the power signals for both motor's phases when a) the power stage is adjusted according to the proposed methodology to the load and b) when only one of the motor's phases (phase 1) is ajdusted to the load. In figure 7a) it can be easily seen that both signals are approximatelly of the same amplitud and the phase lag between them is roughly 90 degrees as should be for properly establishing a travelling wave ultrasonic wave at the motor's stator.

However, in figure 7b) one of the phases (phase 2) was not matched to the electrical impedance of the load. As a direct consequence of this mismatch, the amplitude of the power signal for this phase has been significantly reduced. In addition, the phase lag between the power signals for both motor's phases is drastically increased and both signals are taken nearly out of phase. The impedance matching has been shown to be an unavoidable step in optimizing the driving characteristics of power stages for piezoelectric resonators. For the particular instance of an USRM60 ultrasonic motor, the electrical impedance mismatch between the power stage and te load leads to inefficient operation and increased energy consumption.

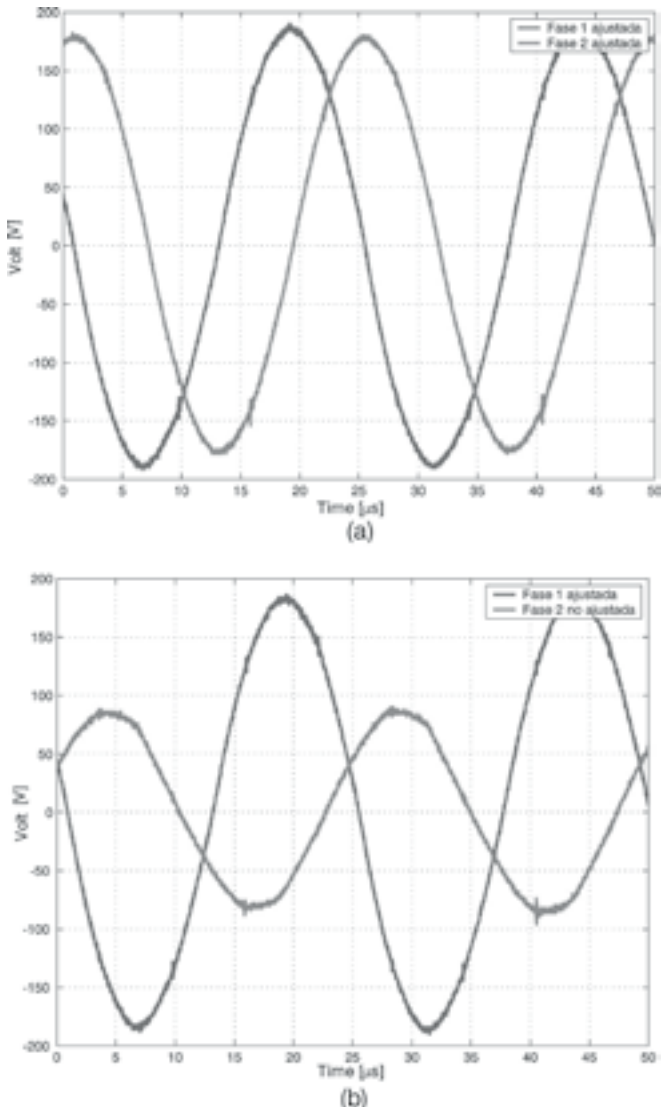

Fig. 7- Comparative analysis of matched and unmatched power signals.

5. CONCLUSIONS

A proper electrical impedance matching between power drivers and piezoelectric resonators is unavoidable to obtain adequate power signals. The energy transfer between the driver and the load improves significantly and so the overall efficiency does.

The right matching of electrical impedance requires a preliminary electromechanical characterization of the piezoelectric resonator, the USRM60 ultrasonic motor in this paper. The determination of these parameters can be approached through combined modal and electrical analysis of the load. This paper validated also the approach to model the motor's phases in the vicinity of resonance according to the equivalent electrical circuit concept.

The power stage impedance matching presented in this paper needs to be performed in combination with intelligent tuning and perturbation rejection strategies at the control stage. By this combinad approach, external perturbations due to load variations or temperature changes can be compensated for and a smooth energy transmission to the load is achieved.

ACKNOWLEDGEMENTS

The authors would like to thank the Spanish Ministry of Education that partially funded this resaerch through grant DPI2002-04180-C02-01.

REFERENCES

1. J.L.Pons, Emerging actuator technologies. A micromechatronic approach, John Wiley & Sons Ltd., Chichester, 2005.
2. J.L. Pons, P. Ochoa, M. Villegas, J.F. Fernández, E. Rocon, Self tuned driving of piezoelectric actuators. The case of ultrasonic motors, X International Conference on Electroceramics, Toledo, Spain, 18-22 June, 2006.
3. D. Mesonero-Romanos, J.F. Fernández, M. Villegas, R. Ceres, E. Rocon, J.L. Pons, Comparación entre excitación resonante y forzada de motores electrocerámicos, Bol. Soc. Esp. Cerám. V., 43, 4, 725-731 (2004).
4. H. Rodríguez, R. Ceres, L. Calderón, J.L. Pons, Modelling of the travelling wave piezoelectric motor stator: an integrated review and new perspective, Bol. Soc. Esp. Cerám. V., 43, 3, 700-707 (2004).
5. S. Ueha and Y. Tomikawa, eds., Ultrasonic motors. Theory and applications, Clarendon Press, 1993.
6. U. Schaaf and H. van der Broeck, Piezoelectri motor fed by a PLL-controlled series resonant converter, European conference on Power Electronics and Applications, September 1995.
7. J.L. Pons, A comparative analysis of Pezoelectric and Magnetostrictive actuators in Smart Structures, Bol. Soc. Esp. Cerám. V. 44, 146-154 (2005).

Recibido: 15.07.05
Aceptado: 01.03.06